New Phytologist

Research

Despite rapid warming, seed production is not leading poleward migration in North American and European forests

James S. Clark[1,2], Taylar Bankston[3], Michal Bogdziewicz[4], Maxime Cailleret[5], J. Julio Camarero[6], Sylvain Delzon[7], Bruno Fady[8], Andrew Hacket-Pain[9], Mick E. Hanley[10], Miao Hu[1], Inés Ibáñez[11], Lauren Jenkins[1], Valentin Journé[12], Roland Kays[13,14], Georges Kunstler[15], Jordan Luongo[1], Anders Mårell[16], Sierra McMurry[13,14], Kira Meyer[1], Emily Moran[17], Thomas A. Nagel[18], Tong Qiu[1], Elena Quintero[19], Miranda D. Redmond[3], Chantal D. Reid[1], Francisco Rodriguez-Sánchez[19], Marie-Claude Bel-Venner[20], Samuel Venner[20], Miguel A. Zavala[21], Shiqi Zheng[1] and Magdalena Zywiec[22]

[1]Nicholas School of the Environment, Duke University, Durham, NC 27708, USA; [2]Department of Statistical Science, Duke University, Durham, NC 27708, USA; [3]Department of Environmental Science, Policy, and Management, University of California, Berkeley, CA 94720, USA; [4]Forest Biology Center, Adam Mickiewicz University, Uniwersytetu Poznaskiego 6, Poznan, 61-614, Poland; [5]INRAE, Aix Marseille Univ, Aix-en-Provence, 13080, France; [6]Instituto Pirenaico de Ecología (IPE-CSIC), Avda. Montañana 1005, Zaragoza, 50192, Spain; [7]INRAE, University of Bordeaux, BIOGECO, Pessac, 33615, France; [8]INRAE, URFM, Avignon, 84914, France; [9]Department of Geography and Planning, University of Liverpool, Liverpool, L69 7ZT, UK; [10]School of Biological and Marine Sciences, University of Plymouth, Plymouth, PL4 8AA, UK; [11]School for Environment and Sustainability, University of Michigan, Ann Arbor, MI 48109, USA; [12]Department of Biology, Faculty of Science, Kyushu University, Fukuoka, 819-0395, Japan; [13]Department of Forestry and Environmental Resources, NC State University, Raleigh, NC 27695, USA; [14]North Carolina Museum of Natural Sciences, 11 West Jones Street, Raleigh, NC 27601, USA; [15]University Grenoble Alpes, INRAE, LESSEM, St-Martin-d'Hères, 38402, France; [16]INRAE, EFNO, Nogent-sur-Vernisson, F-45290, France; [17]Life and Environmental Sciences, University of California Merced, Merced, CA 95343, USA; [18]Department of Forestry and Renewable Forest Resources, Biotechnical Faculty, University of Ljubljana, Ljubljana, 1000, Slovenia; [19]Departamento de Biología Vegetal y Ecología, Universidad de Sevilla, Sevilla, E-41012, Spain; [20]Laboratoire de Biométrie et Biologie Evolutive, UMR 5558, Université Lyon 1, Villeurbanne, 69622, France; [21]Departamento de Ciencias de la Vida, Universidad de Alcalá, Alcalá de Henares, Madrid, 28805, Spain; [22]W. Szafer Institute of Botany, Polish Academy of Sciences, Lubicz, Kraków, 46 31-512, Poland

Author for correspondence:
James S. Clark
Email: jimclark@duke.edu

Received: *3 November 2025*
Accepted: *30 March 2026*

New Phytologist (2026)
doi: 10.1111/nph.71223

Key words: climate change, climate velocity, drought, forest regeneration, late freeze, response velocity, seed production, tree migration.

Summary

- To survive climate change, forest trees will have to shift seed production poleward. However, warming will not stimulate tree fecundity in the north if it is limited by other habitat variables.
- We evaluated the responses of tree fecundity to climate change for 292 tree species in North America and Europe, using response velocity, defined as (climate sensitivity) × (climate-change rate). The sensitivities to climate were estimated for each species and combined with rates of climate change to quantify how temperature, moisture deficits, and late freeze are influencing biogeographic shifts in tree reproduction.
- The results show that moisture deficit and late freeze, not annual temperature, drive changing seed production. Unlike annual temperature, which is increasing generally, change in these climate variables is not driving poleward shifts in seed production.
- These findings do not challenge the expectation that forests might eventually shift poleward. Rather, they show why current efforts offer divergent interpretations. The changes happening now are not consistent with annual temperature trends. As warming continues, fecundity changes can best be anticipated from temperature interactions with precipitation and extremes that impact flowering and fruiting in winter and spring.

Introduction

If migration is to sustain species at risk from rapid climate change, it has to start with seed production. Climate mitigation efforts aim to facilitate the spread of populations poleward as the planet warms (Williams & Dumroese, 2013; Bower *et al.*, 2024). Where active reforestation is feasible in the United States, Canada, and Europe (EU), it is increasingly guided by temperature-driven species projections (Linnakoski *et al.*, 2019; Lieffers *et al.*, 2020; MacKenzie & Mahony, 2021; USDA Forest Service, 2022; Lima *et al.*, 2024), but field evidence does not agree on where tree migration is occurring naturally or, if not, why not. The question remains: If populations lag behind rapid warming, by how much and why? The diverse effects of climate

on seed production, establishment, growth, and survival (Körner & Hiltbrunner, 2018) could limit species distributions in diverse ways (Zhu *et al.*, 2014; Qiu *et al.*, 2021; Sharma *et al.*, 2022). Seed production is especially important because it is the first and probably limiting step for range expansion, but seed production data are too sparse and noisy to estimate trends (Clark *et al.*, 2021). Three missing elements are needed to understand the changes that are happening now: (1) estimates of seed production per forest area across landscapes and over time, (2) alternatives to time-series methods for uneven, noisy data, and (3) allowance for responses to climate variables that are changing at different rates. Here, a new data synthesis is combined with response velocity (Clark *et al.*, 2021; Qiu *et al.*, 2023b), an alternative to current methods that integrates fecundity responses across climate gradients that change in multiple ways simultaneously. Results show how seed production is responding to climate change and why it is not explained by change in annual temperature trends.

Building the space–time evidence needed to understand biogeographic change has been frustrated by data that are difficult to translate between studies and sites. The Masting Inference and Forecasting (MASTIF) initiative provides a first synthesis of seed production per tree and per area on an annual basis (Clark *et al.*, 2021; Journe *et al.*, 2022; Qiu *et al.*, 2023a). The MASTIF network spans species and habitats across North America (NA) and EU (Supporting Information Fig. S1). The modeling approach translates individual fecundity to seed production of all trees on extensive forest inventory plots (Fig. S2) over the last 15 yr.

For population change, an approach is needed that makes use of biogeographic relationships between tree fecundity, climate, and terrain. Traditional time-series methods cannot extract trends that are masked by erratic order-of-magnitude variation from one yr to the next in unevenly distributed observations (Clark *et al.*, 2021). The widely recognized 'masting' phenomenon depends on poorly understood feedbacks that produce volatile annual changes (Pesendorfer *et al.*, 2020; Shibata *et al.*, 2020; Wion *et al.*, 2020; Wright *et al.*, 2021; Qiu *et al.*, 2023a) and obscure decadal trends. Even time series lasting more than a decade may include few mast events (Suzuki *et al.*, 2005). One mast event during a study interval, vs two or three, can profoundly affect trend estimates, depending on whether events come early or late in the series. The distinction between the spatial gradient response and the time-series response is demonstrated with models that decompose climate responses into norms and anomalies (Clark *et al.*, 2014, 2021). Interannual volatility contrasts with emerging evidence for responses across gradients in climate and terrain, which can be spatially smooth (Clark *et al.*, 2021; Sharma *et al.*, 2022).

An alternative to time-series analysis that is widely used to detect population range shifts is based on a species' central tendency in space, obtained by weighting the locations where it is observed by its abundance or performance. These centroids are compared for different time periods or life stages. Because they describe central tendency, geographic centroids cannot shed light on populations that move in multiple directions at the same time. For example, poleward migration would result in fecundity centroids positioned to the north of tree-abundance centroids, but the opposite is observed for most tree species in NA (Sharma *et al.*, 2022). Centroids for recruitment rate (new recruits per area yr^{-1}) have been reported south of adults, consistent with higher turnover in warmer climates, but not with poleward migration (Zhu *et al.*, 2014). Of course, both could occur simultaneously, but climate-induced turnover, not migration, dominates the central tendency. Another study found seedling centroids positioned north of adults for northern but not southern species (Woodall *et al.*, 2009). Comparisons of adult centroids at two time points showed idiosyncratic changes in the eastern United States (Fei *et al.*, 2017), and a shift toward warm-tolerant species in the western United States (Rosenblad *et al.*, 2023). A study of elevation change reported that centroids shift upslope for some species and downslope for others (Rabasa *et al.*, 2013). Efforts to improve the resolution of population margins have expanded from centroids to higher quantiles, for example the latitude delimiting 95% of a population. However, quantiles are still governed by the entire population, not just its margins – expansion or contraction at a margin affects centroids and quantiles alike, regardless of whether there is movement in other margins. Quantile studies report seedling recruitment that is more consistent with contraction than poleward expansion (Nigro *et al.*, 2025), even at cold frontiers (Zhu *et al.*, 2012). Further north, more species than not showed evidence of a poleward shift in sapling and adult quantiles, but still find that adult quantiles are poleward of saplings (Sittaro *et al.*, 2017). Confusingly, centroids or quantiles for demographic rates such as growth can change even when there is no change in the distribution of the species. The conflicting evidence is complicated further by the lack of habitat variables that might explain the differences.

Inconsistent evidence owes not just to methodology, but also to the nature of climate change and the many ways that climate affects recruitment. Both temperature and moisture are important for tree reproduction. Temperature affects bud set, the onset and end of winter dormancy, pollinator activity (Corbet *et al.*, 1993; Alquichire-Rojas *et al.*, 2024), and fruit development (Stephenson, 1981). Beyond annual averages, temperature is important for its extremes and its interaction with precipitation (Thomashow, 1999; Charrier *et al.*, 2021). The freezing temperatures that destroy fruit crops in spring represent an interaction between the timing, duration, and depth of the freeze (Brito *et al.*, 2019; Fernandez *et al.*, 2022; Clark *et al.*, 2026). Moisture deficit is an interaction between precipitation and atmospheric demand – also temperature dependent. Fruit abortion is common during moisture deficits (Stephenson, 1981; Gucci *et al.*, 2009) with documented impacts on fecundity in field studies (Clark *et al.*, 2014; Whipple *et al.*, 2019; Le Roncé *et al.*, 2021). Unlike annual temperature, which is increasing in general, changes in these temperature interactions are regionally complex (Fig. 1).

Response velocity is an alternative approach that exposes the pace at which climate forces fecundity change based on variation across the species range, while allowing for the effects of habitat and individual condition (Clark *et al.*, 2021). It expands the

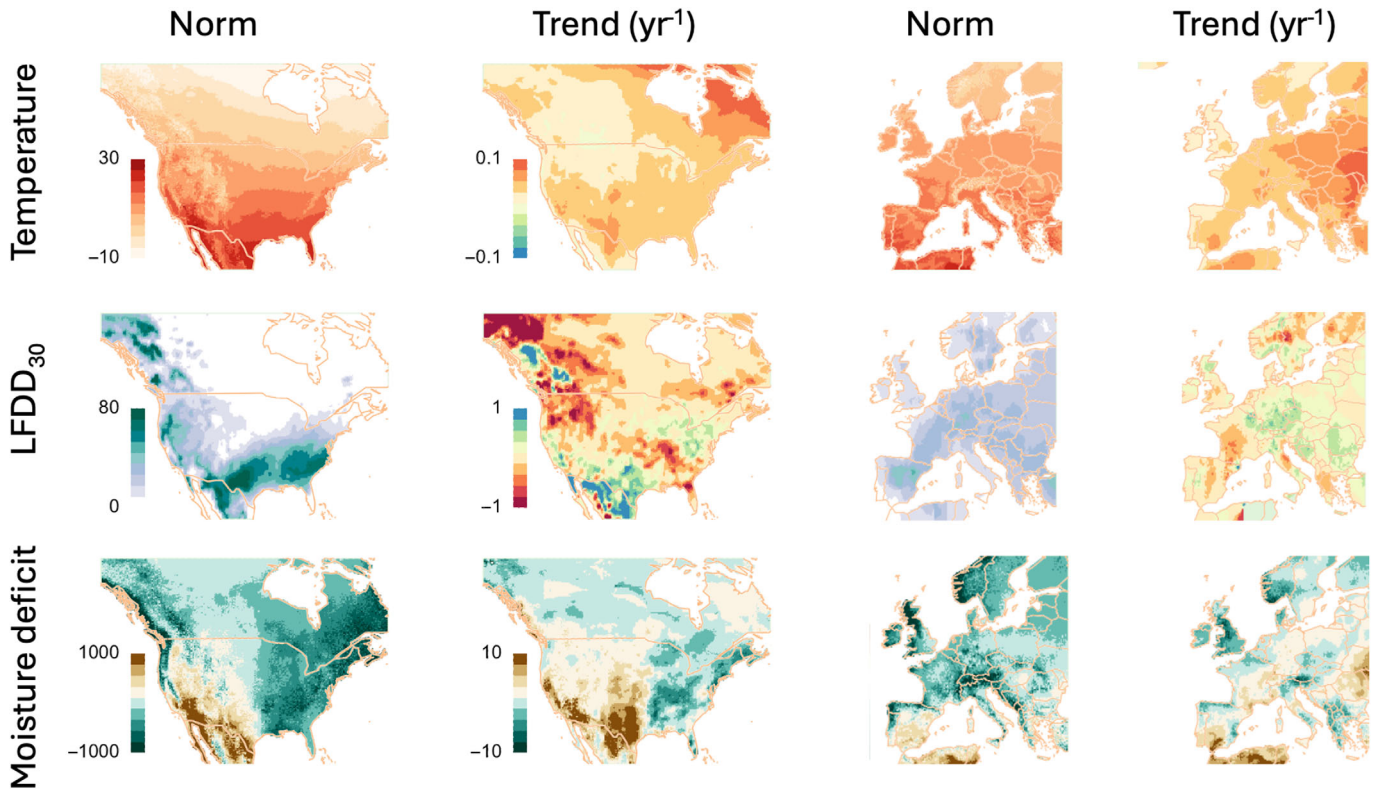

Fig. 1 Climate norms and trends that affect tree fecundity for 15 yr (2010 to 2024). Temperature (top) is trending upward (°C yr^{-1}) across both continents. Trends in late-freeze degree days (LFDD) and moisture deficit D (mm) are regional, including both increases and decreases. LFDD is shown for a chilling delay of CD = 30 degree days (see text). Trends are the forcing terms $\frac{dT}{dt}$, $\frac{dL}{dt}$, and $\frac{dD}{dt}$ in Eqn 5.

concept of climate velocity (Loarie *et al.*, 2009; Schliep *et al.*, 2015; Dobrowski & Parks, 2016), which combines the rate of climate change dC/dt with its spatial gradient over distance X to obtain distance per time, or 'velocity': $\partial X/\partial C \times dC/dt = dX/dt$. Response velocity can be applied to any response variable; here, the response is log fecundity, F. The approach substitutes a biological response to climate, $\partial F/\partial C$, for the climate gradient itself. It is the product of this climate sensitivity and climate forcing dC/dt,

$$\frac{dF}{dt} = \frac{\partial F}{\partial C}\frac{dC}{dt} = \beta_C \frac{dC}{dt}$$
$$= \text{sensitivity} \times \text{climate forcing}$$

(Our use of the terms sensitivity and forcing are consistent with climate science, where forcing refers to change in Earth's energy balance, and sensitivity is the per-unit climate response to that forcing; e.g. Hansen *et al.*, 2025). Here, forcing is climate change, and sensitivity is the per-unit fecundity response. In its simplest form, a model might be fitted as $F \propto \beta_C C$. Then β_C is the sensitivity of F to a changing climate variable C, or $\beta_C = \frac{\partial F}{\partial C}$.

Response velocity is more flexible than suggested by analogy with climate velocity, as it allows for the effects of individual condition, local habitat, and their interactions with all aspects of climate change. We include three climate variables that are changing rapidly across NA and EU and have emerged as important influences on tree fecundity (Clark *et al.*, 2014, 2021; Sharma *et al.*, 2022), temperature T, late freeze L, and moisture deficit D (Fig. 1; Eqn 5),

$$\text{response velocity} = T \text{ forcing} \times \text{sensitivity} + L \text{ forcing} \times \text{sensitivity} + D \text{ forcing} \times \text{sensitivity}$$

The term(s) that dominate response velocity can vary between species and within species geographically due to interactions with other variables (Table 1). The effect of moisture deficit depends on terrain (drainage and solar radiation), so there is a slope × aspect × moisture–deficit interaction. For example, in dry climates, fecundity may be limited by moisture or heat stress and therefore be highest on moist, north and northeast aspects. In moist climates, fecundity may be limited by radiation and thus be high on south aspects. These terrain interactions differ between species (Jenkins *et al.*, 2026).

In this study, we apply response velocity with MASTIF data to test the hypothesis that warming trends across NA and EU (Fig. 1) are driving tree fecundity poleward. Alternatively, an expected range of species' sensitivities to climate variables in Fig. 1 that are not changing everywhere in the same direction could dominate and result in complex regional responses. To test this hypothesis, we model responses to climate while allowing for

differences in tree size, shading from neighbors, soil pH, and terrain. Predictive distributions from the fitted model are then decomposed into the effects of each climate variable, providing insight not only into rates of change but also the variables responsible for them.

Materials and Methods

The analysis quantifies seed production by individual tree-years. It translates those estimates to seed production per forest area. These area estimates, applied to forest inventories distributed across the two continents, are the basis for response velocity. The approach consists of four elements summarized in Fig. 2, including data synthesis, model fitting and prediction, and evaluation of response velocities. Sections that follow summarize observations and modeling elements to supplement those in the text.

Study regions and species

Tree fecundity is estimated from seed-trap (ST) and crop-count (CC) data collected in regions supporting woody vegetation in NA and EU. Biomes include the winter-rain shrub and woodland (Mediterranean) zones in California and southern EU (Fig. S2). Continental interiors include temperate mixed forests, pine sand hills and savannas, and semiarid woodlands. The study extends north to boreal forests and up elevation to the montane and alpine zones of the Cascades, Sierra Nevada, Rockies, Appalachian, Pyrenees, and Alps.

The analysis includes woody plant species, both angiosperms and gymnosperms, that are abundant enough to estimate fecundity (Fig. 3). This excludes Salicaceae, which are rarely recovered in STs and not amenable to CCs. This includes 198 species in NA and 94 species in EU, representing 31 families and 76 genera (Fig. S3).

Table 1 Covariates used to fit the Masting Inference and Forecasting (MASTIF) model and data sources.

Covariate	Units	Minimum data range	Minimum Data SD	Data source
Tree diameter ($G_{ij,t}$, $G^2_{ij,t}$)	cm, cm^2	>1 cm	3 cm	MASTIF[1]
Shade class ($B_{ij,t}$)	Ordinal (class 1–5)	3 classes	2	
Moisture deficit norm (D_i)	mm	100 mm	40 mm	terraClimate[2], CHELSA[3]
Deficit anomaly ($D^a_{i,t}$)	mm	50	20	terraClimate, CHELSA
Temperature norm (T_i, T_i^2)	°C	5°C	3°C	terraClimate, CHELSA
Temperature anomaly ($T^a_{i,t}$)	°C	53°C	3°C	terraClimate, CHELSA
Late-freeze norm (L_i)	DD	20 DD	5 DD	Daymet[4], ECAD[5]
Late-freeze anomaly ($L^a_{i,t}$)	DD	20 DD	5 DD	Daymet, ECAD
pH$_i$ (0–30 cm)	Log concentration	1	0.2	soilgrid250m[6]
Slope (S_i)	m m^{-1}	0.05 m m^{-1}	0.03 m m^{-1}	DEM[7]
Slope × Aspect[8]	m m^{-1}			
Slope × Aspect × Deficit[9]	m m^{-1} × mm			
Topographic position (P_i)	m	40 m	4 m	
Ecoregion (for year effects)	Categorical			World Wildlife Fund[10]

Subscripts are tree i, site j, and year t. Norms are for the 15-yr period from 2010 to 2024. Annual anomalies have the superscript a. Variable selection results in a subset of these predictors for each species. The data range and SD requirements determine whether to include a predictor in the fitted model; if there is not meaningful variation, an estimate may be significant but misleading. Subsequent variable selection is by deviance information criterion (DIC) (Clark *et al*., 2019). [1]Clark *et al*. (2021); [2]Abatzoglou *et al*. (2018); [3]Karger *et al*. (2017); [4]Thornton *et al*. (2022); [5]Cornes *et al*. (2019); [6]ISRIC (2024); [7]Gesch *et al*. (2002); [8]Two terms: $S_i(\sin A_i, \cos A_i)$ for slope S and aspect A in radians. [9]Two more terms: $D_i S_i(\sin A_i, \cos A_i)$. [10]Year effects are grouped by ecoregion Olson *et al*. (2001).

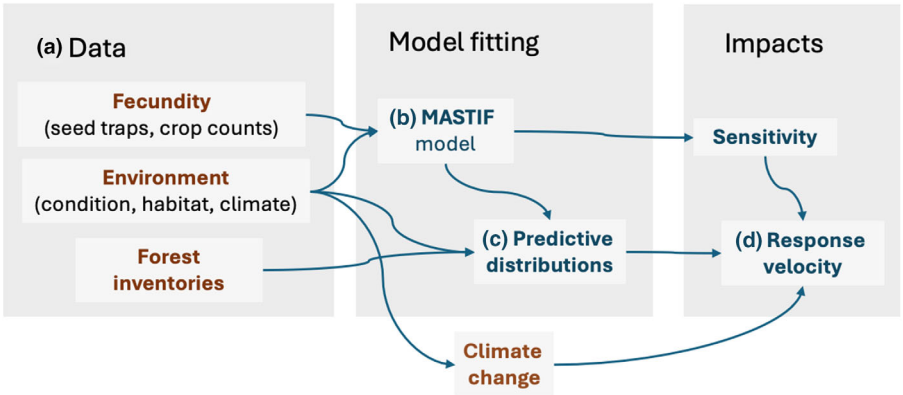

Fig. 2 Analysis consists of data collections (a), model fitting (b), and generation of predictive distributions for forest inventory plots (c), and evaluation of response velocities (d).

Fig. 3 Capacity to move with climate change depends not only on dispersal, but also on fecundity. Response velocity quantifies how the pace of climate change influences fecundity change, which need not associate with traits that influence dispersal, including movement by scatter-hoarding rodents (a), a wide range of vertebrate consumers (b), and wind (c).

MASTIF data and model

We summarize key elements from the complete description of model fitting, diagnostics, and prediction detailed in, for example, Clark *et al.* (2019) and Clark *et al.* (2021). The MASTIF analysis differs from other compilations of tree fecundity in four ways. First, analysis is restricted to data that reference the amount of seed produced by a tree in a given year. We exclude studies based on ordinal summaries (e.g. 'low', . . ., 'high') or seed counts per time, the latter bearing a nonlinear relationship with the actual seed produced (the higher the production, the smaller the fraction observed). We do not include studies that use ST counts to directly estimate seed production per area because they are dominated by a few nearby trees – they do not represent the stand.

MASTIF data include STs and CCs. ST data used in MASTIF come from mapped inventory plots where seed production can be modeled from tree condition and tree-to-trap distances (Clark *et al.*, 2004; Muller-Landau *et al.*, 2008; Moran & Clark, 2011). In the MASTIF model, ST counts are conditionally Poisson depending on the production of individual trees, their collective distances from seed traps, and identification errors (Clark *et al.*, 2019); seeds may be miss-identified or identified only to genus. The Poisson intensity for counts of seed type m in trap k is

$$\text{seed trap count}_{mk} \sim \text{Poi}\left(\text{trap area}_k \times \sum_i \left[\text{dispersal from } i \text{ to } k \times \text{species}_i \text{ counted as type}_m \times \text{true crop}_i\right]\right) \quad \text{Eqn 1}$$

for all trees $i = 1, \ldots$ on an inventory plot. Model fitting includes a seed dispersal (re-distribution) kernel and an error matrix (probability that species i is recorded as seed type m). CCs of observed fruit on a tree are recorded with an estimate of the fraction of the entire crop that is observed, or crop fraction (CF). CC data are conditionally beta-binomial,

$$\begin{aligned}\text{crop count}_i &\sim \int_0^1 \text{binom}\left(\text{true crop}_i, \text{CF}_i\right) \\ &\quad \times \text{beta}\left(\text{CF}_i | a_i, b_i\right) d\,\text{CF}_i \\ &\sim \text{beta-binomal}\left(\text{true crop}_i, a_i, b_i\right)\end{aligned} \quad \text{Eqn 2}$$

Parameter values $(a, b)_i$ describe a beta distribution for individual i with mean value CF_i and allow for the increasing uncertainty in CF_i as its value approaches zero (Clark *et al.*, 2019). Through its influence on estimated latent fecundity, the spread in an individual's CC distribution affects its contribution to estimates of sensitivity coefficients. Although ordinal data are excluded, the model accommodates censored data, both for ST and CC counts within intervals, such as (0, 1, 2–5, 6–20, > 20) in (Bourg *et al.*, 2013).

A second difference is the use of a hierarchical Bayes state-space model to accommodate dependence between trees, within trees over time, and between seed traps. Seed production in 1 yr depends on previous years (e.g. the masting phenomenon). This year-to-year dependence violates the assumption of independent observations. ST counts are dependent because traps collect seeds from many of the same trees. In the MASTIF model, tree maturation status and fecundity are latent variables that allow for these sources of dependence (Clark *et al.*, 2019). In addition to the effects of predictors, the model includes random individual effects and year effects assigned to each ecoregion, the latter approximating the regional scale where quasi-synchronous masting can emerge. CC data can be time series for trees observed repeatedly or opportunistic one-time counts. In the latter case, there is no random individual effect (the individual is observed once), and the variance between individuals is marginalized into the process error that is part of the process model (see Eqn 3). Model fitting used the MASTIF package in R.

The third difference is that climate predictors are decomposed into spatial and temporal effects. The climate effects on individuals that experience different climate norms are confounded with climate variation over time. Decomposition into norms and anomalies (Table 1) allows estimation of both effects (Clark *et al.*, 2014, 2026).

The fourth difference is that the fitted fecundity model is combined with inventory data to estimate seed production per forest area (Clark *et al.*, 2021; Journe *et al.*, 2022; Sharma *et al.*, 2022). The same predictors are available for fitted trees and trees on inventory plots (Table 1). The predictive distribution for each tree each year on plots of known area provides the seed production per area used to evaluate response velocity. All woody plants with sufficient data coverage are included in the model (Fig. S3).

Predictors enter the model through maturation status and fecundity conditional on being reproductively mature. Both data types in Eqns 1 and 2 are conditional on the 'true crop', which is the seed produced by a tree in a given year. To summarize the model detailed in Clark *et al.* (2019), seed production f occurs for a tree that is reproductively mature, $m = 1$, as $[f, m = 1] = [f|m = 1][m = 1]$, where mature status is a probit function of tree diameter (Clark *et al.*, 2019). Fitted coefficients include main effects of predictors (including norms and anomalies for moisture deficit (MDEF) and late-freeze degree days (LFDD), interactions, and year effects). The conditional fecundity model for tree i at location j (within eco-region r) in year t is'

$$\log f_{ij[r],t} = \mathbf{x}'_{ij,t}\boldsymbol{\beta} + \gamma_{r,t} + \alpha_i + \epsilon_{ij,t} \qquad \text{Eqn 3}$$

where $\mathbf{x}_{ij,t}$ is the design vector holding main effects and interactions, $\boldsymbol{\beta}$ is the corresponding vector of fitted coefficients, $\gamma_{r,t}$ is the year effect for ecoregion r, α_i is the random effect, and $\epsilon_{ij,t}$ is random error. The year effect takes up synchronous variation between trees of an ecoregion that are not explained by interannual climate anomalies.

Predictors in the model are broadly consistent with the masting literature that has focused on winter/spring conditions and growing season moisture, while at the same time minimizing model size. Climate variables are defined for months that are important for reproduction in a given year. Annual temperature is included in the model because it is central to the literature on tree migration and because all months can contribute to seed production, albeit in different ways (Körner & Hiltbrunner, 2018). We include months from the previous and current years through the time of fruiting. We allow for a quadratic response (hump-shaped) response. LFDD summarize risks at the time of flowering and fruiting, when development is especially vulnerable to low temperatures. For late freeze, chilling days accumulate from December of the previous year until the chilling delay is satisfied, followed by LFDD accumulation until freezing temperatures no longer occur (Clark *et al.*, 2026; see Supporting Information). Growing season moisture deficits threaten seed crops to the extent that fruit abortion is common in dry years (Stephenson, 1981; Charrier *et al.*, 2021). Although effects can be acute in summer, soil moisture levels integrate variation in precipitation from the previous year. We include the accumulated difference between monthly PET and P from the previous and the current year until seeds are developed. This current year contribution runs through May for spring-dispersed seed (*Acer, Ulmus*) and through August for all others. Our deficit variable allows for moisture excess, in the sense that PET – P can be negative when precipitation (P) exceeds potential evapotranspiration (PET). Climate variables are included as the local site norm and the site anomalies (Clark *et al.*, 2013).

In addition to climate, predictors include individual attributes (diameter and shade class – see Supporting Information: Shade class), soil pH, and terrain (slope, aspect and topographic position). These shape variables are used instead of solar irradiance because the latter does not integrate how terrain can affect drainage, heat load, and insolation. We include the interaction between terrain and moisture deficit because moisture and insolation effects can be amplified by climate (Jenkins *et al.*, 2026).

Climate sensitivity estimates $(\widehat{\beta}_T, \ldots)$ in Eqn 5 are available for variables that are retained following variable selection, as detailed in Clark *et al.* (2019). Because species differ in geographic ranges and sampling, initial screening restricts the model (terms in Table 1) to those with sufficient absolute range and SD, shown in Table 1, and with variance inflation factors < 10. The selected model for each species has the lowest DIC. Model diagnostics are included for all fitted models and Bayesian SE in Supporting Information.

Continental prediction Predictive distributions of seed mass follow methods of Clark *et al.* (2021), see also Sharma *et al.* (2022), Qiu *et al.* (2021) and Journe *et al.* (2022). Combining the production of all trees on a plot yields fecundity per area per year for $> 10^5$ plots in NA and EU (Supporting Information). In NA, inventory plots include United States Department of Agriculture (USDA)'s Forest Inventory and Analysis (FIA) program, NEON, and Canada's National Forest Inventory (NFI). In EU, inventory plots come from country-based national inventories. On both continents, national inventories are supplemented with fixed-area and variable-radius plots in the MASTIF study (Supporting Information). Plots vary in size and in the minimal diameter used to include trees. We exclude trees below 12 cm in diameter to make plots comparable. Few trees below this size threshold are reproductive, so the effect of this threshold is small. Species-level parameter estimates are available for 87% of trees that occur on inventory plots, the remainder summarized by genus-level estimates (Supporting Information).

Response velocity and trends The terms in response velocity that change or interact with variables that change are temperature T (°C), late-freeze degree days L (degree days), and moisture deficit D (mm per month),

$$E(F) = \overbrace{\beta_T T + \beta_{T^2} T^2}^{\text{temperature}} + \overbrace{\beta_L L}^{\text{late freeze}} + \underbrace{\left(\beta_D + \beta_{A_1 D} A_1 + \beta_{A_2 D} A_2\right) D}_{\text{moisture deficit} \times \text{terrain}} + \ldots \qquad \text{Eqn 4}$$

for slope S (m m^{-1}), and aspect variables $(A_1, A_2) = S(\sin A, \cos A)$ for aspect A (radians; Clark, 1990).

Ellipses in Eqn 4 represent terms in the model that do not interact with changing T, L, or D, including model error. The response velocity is the time derivative of Eqn 4,

$$\frac{d}{dt}E(F) = \overbrace{\frac{\partial F}{\partial T}\frac{dT}{dt}}^{\text{temperature}} + \overbrace{\frac{\partial F}{\partial L}\frac{dL}{dt}}^{\text{late freeze}} + \overbrace{\underbrace{\frac{\partial F}{\partial D}\frac{dD}{dt}}_{\text{main effect}} + \underbrace{\frac{\partial F}{\partial (SAD)}(A_1 + A_2)\frac{dD}{dt}}_{\text{terrain interaction}}}^{\text{moisture deficit}}$$

$$= (\beta_T + 2\beta_{T^2} T)\frac{dT}{dt} + \beta_L \frac{dL}{dt} + (\beta_D + \beta_{A_1 D} A_1 + \beta_{A_2 D} A_2)\frac{dD}{dt} \quad \text{Eqn 5}$$

The second line in Eqn 5 substitutes fitted sensitivity coefficients (β_T, ...) for derivatives in the first line. The terms include quadratic temperature effects followed by the main effect of moisture deficit and its interaction with slope : aspect $S(A_1, A_2)$. Thus, although slope and aspect are static, they modulate the response to changing moisture deficit.

For comparison with response velocity, fecundity trends are taken as the slope of the time series (e.g. Hansen *et al.*, 2025). For each species and inventory plot *sj*, the slope is $\mathrm{cov}(\mathbf{F}_{sj}, \mathbf{Y})/\mathrm{var}(\mathbf{Y})$, for log fecundity and year vectors for the 15-yr period from 2010 to 2024. This time interval was selected because it is most recent, sufficiently long to capture trends, and in alignment with most of the fecundity data. This interval is broadly consistent with longer-term trends. One departure is the late-19th century 'warming hole' in the southeastern United States, which has since disappeared (Meehl *et al.*, 2015), hence the positive trend since 2010 (Fig. 1). To evaluate response velocity, the terms of Eqn 5 were assembled from sensitivity coefficients (β_T, ...) and rates of climate change (dT/dt, ...; trends in Fig. 1). The contributions of terms to response velocity were taken as the fraction of variance they represent in Eqn 5.

Results

Seed production is not associated with trends in temperature, but rather with climate variables that changed in different directions. Since 2010, temperatures increased slower in NA than in EU, which were highest in southern Iberia and the east (Fig. 1). In contrast to pervasive warming, change in late freeze and moisture was heterogeneous. Late-freeze norms are higher in southern and western NA than in EU; however, late freeze increased in southern and eastern NA and central and eastern EU, but decreased elsewhere (Clark *et al.*, 2026). In NA, moisture deficits increased in the West and decreased in the East. The western Mediterranean and eastern EU dried rapidly, while northwestern EU and northern Italy saw increasing moisture surpluses.

Trends and response velocities

Response velocities for 292 species in NA (Table S2) and EU (Table S3) combine sensitivities and rates of change in climate (see Materials and Methods section). Fit diagnostics and parameter estimates are available in the Datasets S1–S3 with metadata in Tables S4 and S5. Trend analysis and response velocity represent different variables (change over time vs climate sensitivity × climate change), yet their ranges of variation are similar (lower panels in Fig. 4), albeit with more extreme values in NA. Again, both have the same dimensions: log fecundity per area per year. Trend estimates are degraded by volatile seed production between years, whereas response velocity integrates variation across the range. The distributions for both quantities are concentrated within the interval (−0.1, 0.1), or ±10% fecundity change per year. The zero-centered distributions indicate approximate balance for increase and decrease; 94% and 96% of species include zero within their 95% distribution across NA and EU, respectively (Figs S4, S5).

When averaged separately for species that increase or decrease, North-American trends and velocities were highest in the Southeast and Upper Midwest (Fig. 4). To generate these maps, we determined the overall trend and response velocity by species (Figs S4, S5) and divided them into 'increasers' or 'decreasers'. In EU, the highest fecundity trends and velocities occurred in SW Iberia.

In neither continent are aggregate trends precisely associated with any one climate variable in Fig. 1. However, regions of high response velocity overlap with rapid change in moisture deficit and late freeze. Despite general agreement when averaged across all species, aggregated values in Fig. 4 mask high variation between species.

Sensitivity to climate

Habitat variation is one of two components that contribute to Fig. 5(a), the other being sensitivity. Species sensitivity coefficients, the derivatives in Eqn 5, are detailed in Supporting Information and summarized in Fig. 5(b). For all three climate variables, the ranges of sensitivity coefficients are similar between continents. These sensitivities cannot be compared between variables because they have different units. However, responses to each variable can be compared between continents (they are unstandardized). Positive and negative values are estimated for moisture deficit and late freeze, depending on species. A hump-shaped temperature response has positive linear (β_T) and negative quadratic (β_{T^2}) coefficients. Sixty five percent and 76% of species in NA and EU, respectively, include a nonzero quadratic term (gray bars for $\beta_{T^2} < 0$ in the accepted model), but this does not ensure that a temperature optimum exists within the species range. Although few species show temperature sensitivity on both continents, sensitivity to moisture deficit is more pervasive in NA.

The sensitivity coefficients of Fig. 5(b) combine with the variation in predictors to determine response velocity (Eqn 5). Temperature change is weakly associated with tree fecundity, which aligns instead with moisture deficit and late freeze (Fig. 5a). Terrain modulates moisture stress (orange portion of brown deficit bars), but its importance varies between species. For many species, omission of terrain would miss the effects of moisture deficit on fecundity. Late freeze (blue) follows in importance the

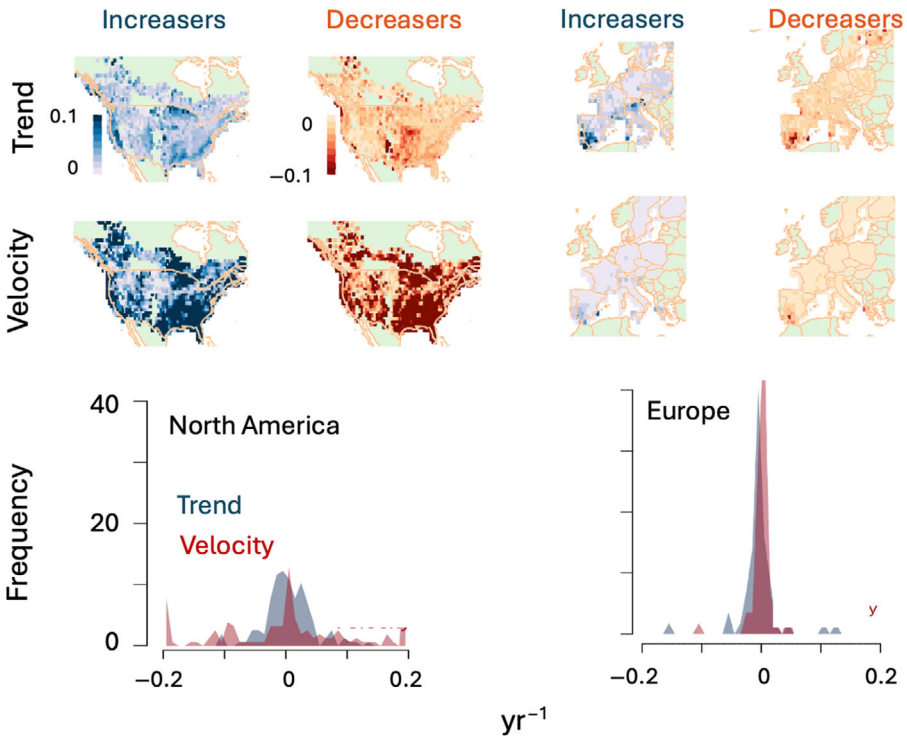

Fig. 4 Trends and response velocities, shown separately as averages for species that had increasing fecundity (blue maps) and decreasing fecundity (red maps). Trends and velocities are aggregated over species at the bottom. The similarities between trend and velocity in these aggregate maps disappear at the species level due to high noise in time-series data used to estimate trends (Supporting Information Figs S4, S5).

moisture deficit, while temperature (black) plays a minor role. The connection to response velocity follows with an example.

Quercus alba (white oak), widespread in eastern NA (Fig. 3), shows the 'hump-shaped' temperature response commonly assumed in species distribution and demographic models (brown in Fig. 6a). This response is evident along the geographic transect of maximum temperature change (inset map). Temperature declines 10°C from southwest to northeast (black line in Fig. 6a). The effect of temperature on fecundity (brown in Fig. 6a) has its maximum near latitude 38° N. Temperature has increased fastest in the deep South and between 39° N and 43° N (black line in Fig. 6b). Because temperature increases across the entire transect, its effect is positive north of this maximum and negative south (brown in Fig. 6b). Again, this is the response shape that should drive poleward migration. In this analysis, many species do not respond in this expected way, in part because the evidence for a hump is absent, but more importantly, temperature effects are overwhelmed by moisture deficit and late freeze.

Despite the hump-shaped temperature response in *Q. alba*, seed production is not shifting poleward because annual temperature is not the dominant contributor to fecundity change. Fig. 6(d) shows the full response decomposed by the three terms in Eqn 5. All three climate variables have changed substantially since 2010 (Fig. 6c), but *Q. alba*'s high sensitivity to moisture deficit made this variable most consequential. Moisture deficit has been declining in the Southeast (negative values in Fig. 6c), associated with fecundity increases do not occur in the northern part of its range. The trend toward increased moisture combined with high sensitivity accounts for its dominating influence on response velocity in Fig. 6(d). Other terms are minor, including the terrain interactions with moisture deficit (orange in Fig. 6d). Although not important for *Q. alba*, terrain interactions are common on both continents (Fig. 5a). Rather than poleward increases in fecundity, the mapped response in Fig. 6 increases in the south (black) and decreases in much of the north (red). Taken across all species, there is no tendency for species velocities to increase poleward because, as for *Q. alba*, temperature effects are dominated by other climate variables Fig. 5.

Although median trends and response velocities show no phylogenetic signal when combined with other ecological traits, their variability (SD) emerge as significant for one of five indices, Pagel's λ (Table S1). In the barplots sorted by phylogeny in Fig. 7, variation is low for response velocity with the exception of a few species in *Pinus*, *Quercus*, *Acer*, and Rosaceae, all from NA. These high values account for the extremes summarized in Fig. 4. Of course, the capacity to identify phylogenetic signal depends on the distribution of data, which will change as data continue to accumulate.

Discussion

The poleward shift in fecundity that is expected from rising temperatures is not observed in NA and EU because seed production is primarily associated with moisture and spring conditions, neither of which generates poleward forcing. Unlike mean annual temperature, which is increasing across both continents, moisture deficits and late freeze show regional increases and decreases (Fig. 1). The locations of rapid fecundity change do not align with rapid temperature increase, because the temperature influence is weak (Fig. 5). The heterogeneous forcing by moisture deficit and late freeze is consistent with the ambiguous movement of centroids in eastern NA (Fei *et al.*, 2017), as is the association

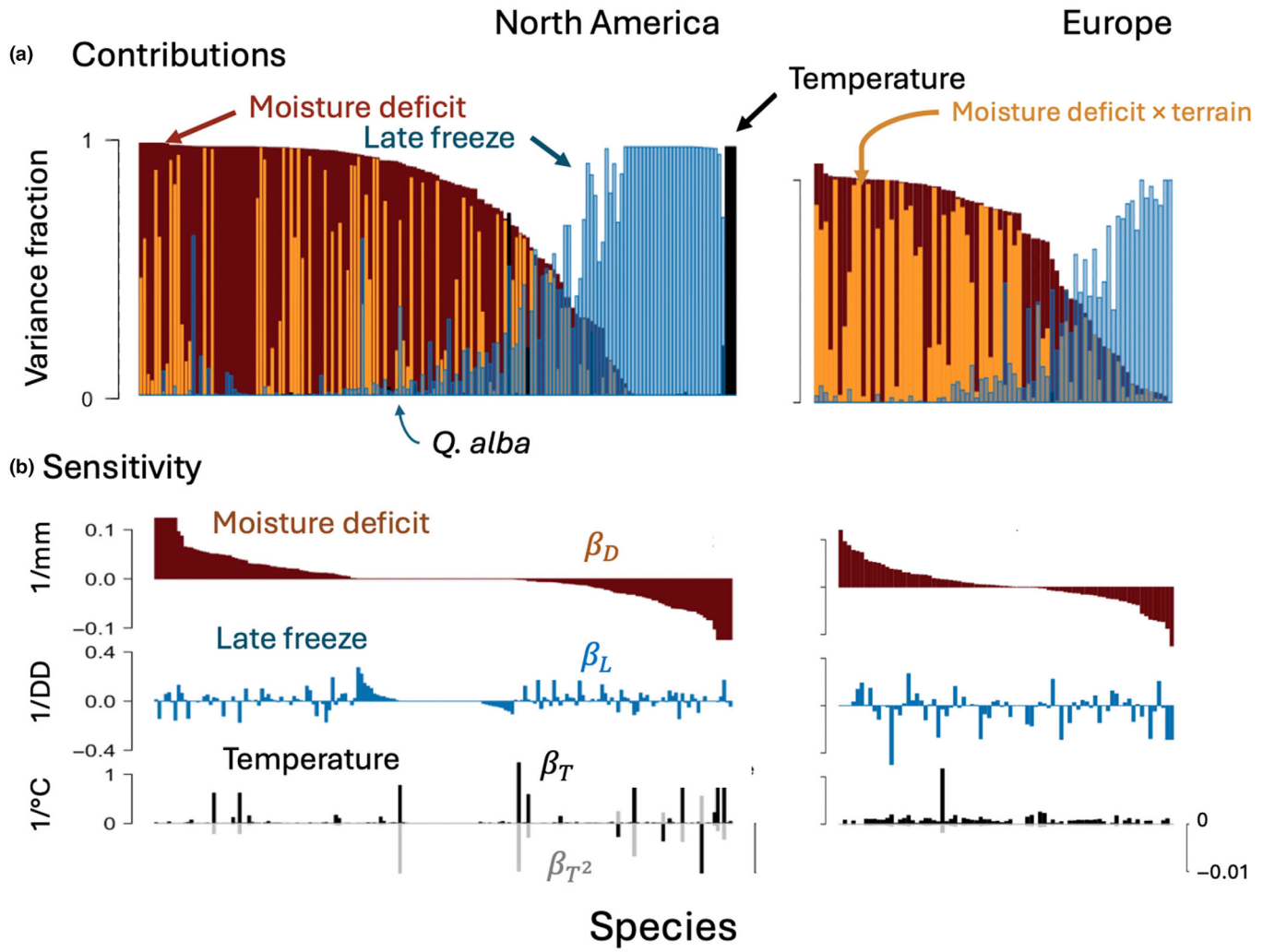

Fig. 5 Variance contributed to response velocity and sensitivity coefficients. (a) Forcing (contribution to response velocity) is dominated by moisture deficit (brown) followed by late freeze (blue; the moisture deficit scale is truncated at (−0.1, 0.1); otherwise, interior values would not be visible due to high values at the extremes). Each vertical line is one species ordered by response to moisture deficit and then late freeze. The moisture–deficit interaction with terrain (slope : aspect) is shown in orange. *Quercus alba*, labeled at left is expanded in Fig. 6. (b) Coefficients from Eqn 5 are species' sensitivities to climate variables, in this case ordered by moisture deficit. Coefficients have similar magnitudes on the two continents, but overall more extreme values in North America. The full table of coefficients and SE is included in Supporting Information.

between aridity and recruitment/adult centroids in western NA (Rosenblad *et al.*, 2023; Nigro *et al.*, 2025). Large changes in southern Iberia (Fig. 4) are associated with declines in moisture that align with orchard losses in NA and EU (Clark *et al.*, 2026).

As with any effort to tie demographic variation to environment, the legacy of past extremes that deteriorates individual condition will be hard to extract from observational data (Pederson *et al.*, 2014; Losso *et al.*, 2022). Efforts have been made to correlate demographic rates with hundreds of lagged interactions in climate data without yielding general relationships. In the species *Homo sapiens*, where clinical and epidemiological data are comparatively enormous, long-term health outcomes remain an area of active research. Just as tree mortality often follows decades of morbidity (Wyckoff & Clark, 2002), we expect that fecundity will likewise reflect past events that will be hard to isolate. Our focus on associations with recent climate variation (current and previous year) attempts to capture effects that might be most consequential.

This study does not find an overall decline in tree fecundity on either continent. For > 90% of species, the locations where fecundity is declining are offset to varying degrees by increases in other regions. Zero-centered distributions of fecundity change (Figs S4, S5) would be expected if, for example, a poleward shift results in increases at high latitudes balanced by declines at low latitudes. This is the conditional effect of temperature on fecundity shown in Fig. 6(a). However, current (and future) habitat availability does not span the full range of climates and terrain that a species might occupy, an issue discussed by Feeley & Silman (2010). For example, the southern ranges of many species are truncated by water bodies (Gulf of Mexico and Mediterranean Sea). East–west trending Mediterranean climates that penetrate to

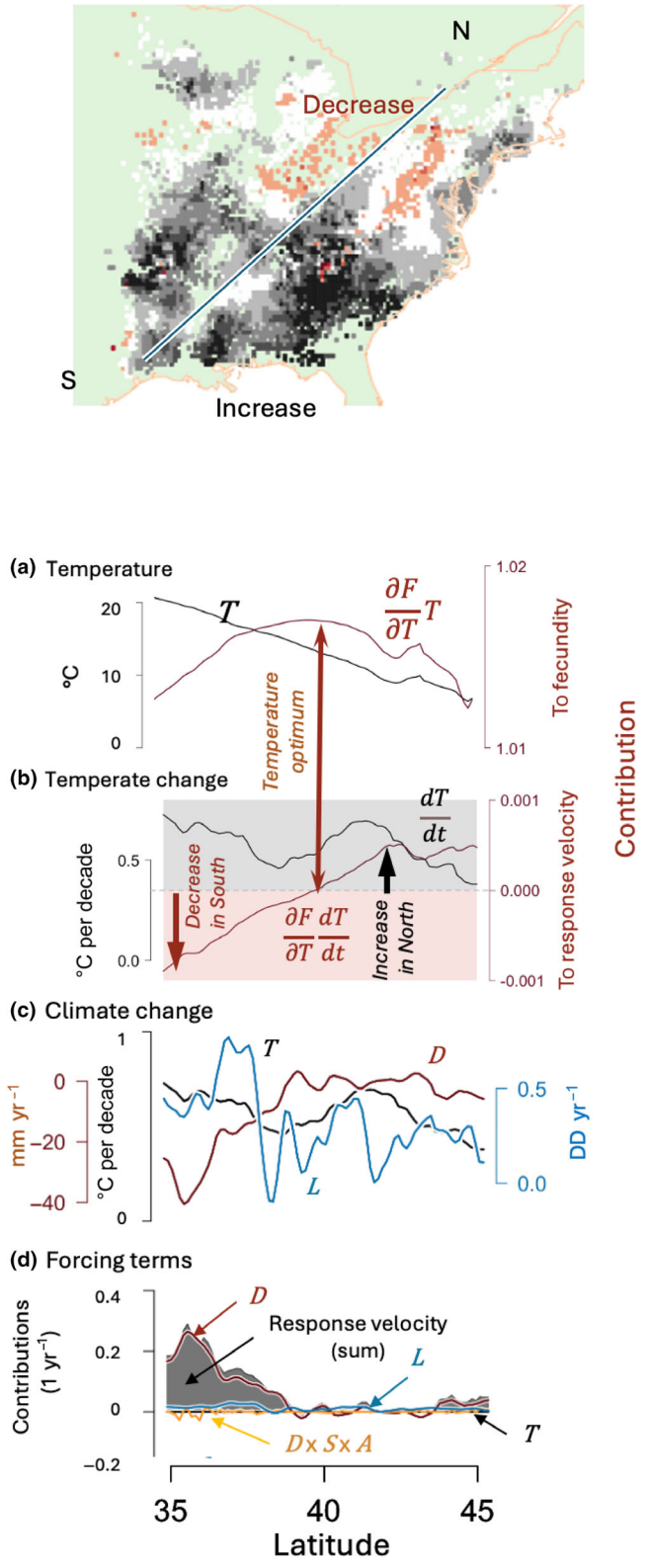

Fig. 6 Climate contributions for *Quercus alba* along the axis of maximum temperature (*T*) change (map) show increases in the South (black) and decreases in the North (red). (a) *T* declines with latitude (black) while its contribution to response velocity increases and then declines (brown). (Terms from Eqn 5) (b) *T* increased at different rates on the transect (black line). Poleward forcing (brown line) comes from a negative contribution South (below the optimum) and positive North. (c) Rates of change corresponding to factors in Eqn 5. (d) Response velocity (shaded gray) is the sum of four terms in Eqn 5; moisture deficit (*D*) dominates. Its interaction with slope:aspect is negligible as are *T* and *L*.

Asia define southern limits for many of the mixed forest species of central EU where conditions are not only warm, but also shift to winter rain. This seasonality shift does not influence southern range limits in eastern NA, which instead trend toward high temperatures and high year-round precipitation before truncation by the Gulf of Mexico. For this reason, southern boundaries for many species cannot be defined solely by temperatures. Potential habitat extends beyond what is offered by geographic constraints and climate/terrain interactions. Although the biogeography of the change in fecundity is not consistent with poleward migration, the apparent balance between increases and decreases is influenced by potential habitat.

As with any observational study, results depend on the distribution of data. The history of observations across two continents that combines opportunistic sampling and long-term inventories offers insights that depend on where species can be observed. Coverage differs for each species (Fig. S1), not only due to geographic constraints on species distributions but also the feasibility of data collection. The estimates offered here will continue to improve as data accumulate.

This analysis does not find clear associations between response velocity and traits that are routinely measured in ecological studies (Fig. 3). The fact that seed size and dispersal vector (animals vs wind) are not closely aligned with response velocities (Table S1) is not unexpected, because dispersal affects fitness whether or not climate is changing, and response velocity is specific to the combination of climate variables that are changing at a time and place. Species represent many combinations of traits that affect the two elements of tree migration, seed dispersal, which influences movement, and response velocity, which affects how fecundity responds to climate change. Species that contrast in traits associated with dispersal (Fig. 8) can have response velocities that average near zero across the map. Most of the abundant small, winged samaras of *Liriodendron tulipifera* (Fig. 3b) move outside of the canopy area of parents (beyond 10 m); they can travel long distances. Unlike most Fagaceae, *Carya* lacks known long-distance dispersers, the woody shell being apparent primarily to rodents (beneath the outer leathery pericarp in Fig. 3b). Without animal dispersal, *Carya alba* has limited migration potential, which could be problematic under rapid climate change. These species with similar ranges of response velocities are expected to differ in migration potential due to dispersal differences. It should be noted, however, that both genera disappeared from western EU when advancing glaciers required spread across challenging terrain that barred entry to southern EU (Orain *et al.*, 2013; Chen *et al.*, 2019).

The potential for greater uncertainty in North-American redistribution is raised by the more extreme response velocities

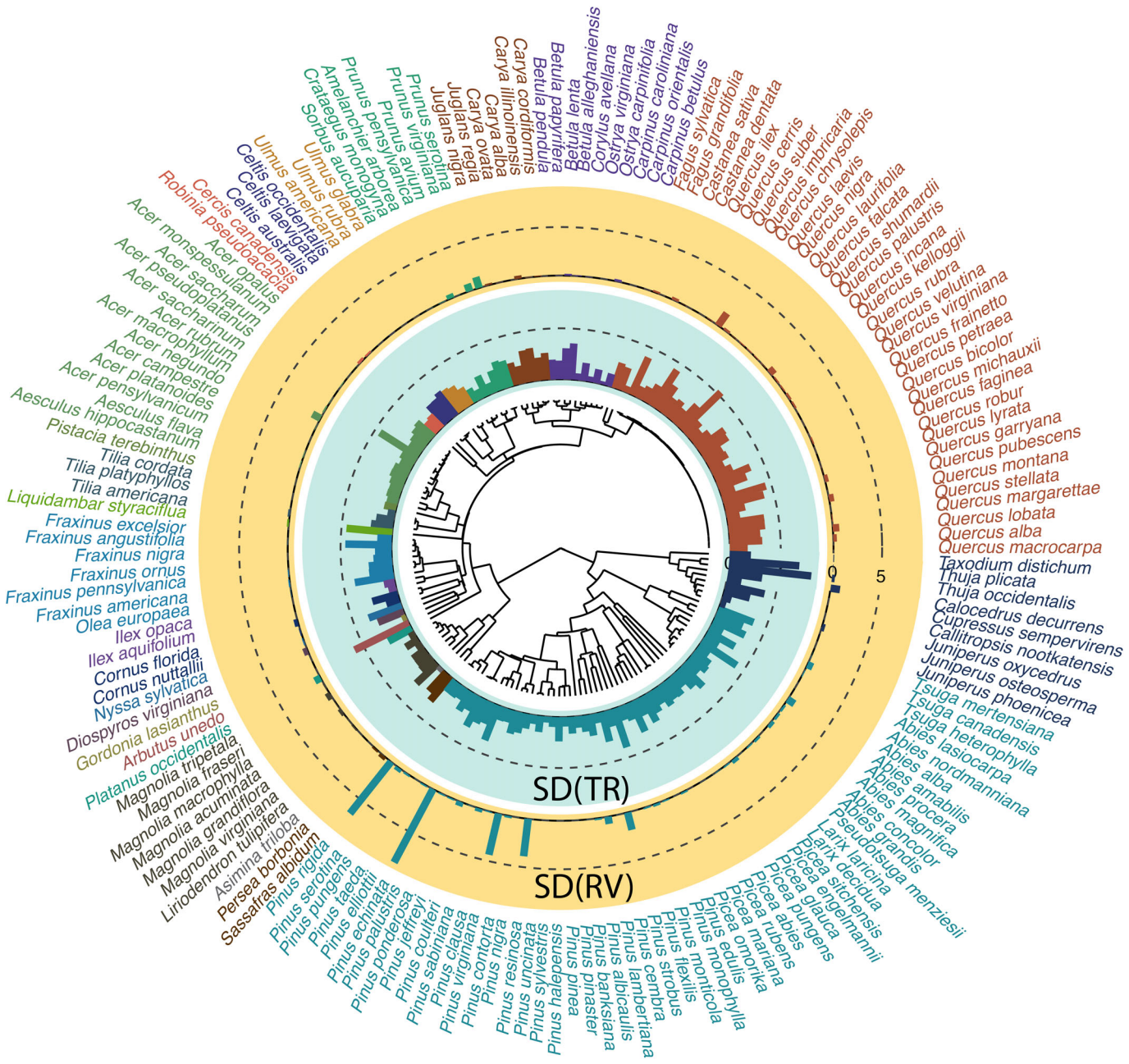

Fig. 7 SDs for trends and response velocities (SD(TR), SD(RV), respectively) show weak relationships to phylogeny (Supporting Information Table S1). With the exceptions of some high values for species in *Quercus* and *Pinus*, variation in RV is much lower than in trends. Colors highlight family differences.

and trends in NA compared with EU (Fig. 4). These extremes might be due to high sensitivities of North-American species (Fig. 5b) and especially rapid change in North-American moisture deficits and late freeze (Fig. 1). It is also possible that more intensive management in EU has degraded relationships between climate and species responses to a greater degree than in NA.

Results do not challenge the expectation that forests will at some point shift poleward. Rather, they show that the changes in fecundity happening now are not consistent with annual temperature trends. As warming continues, temperature effects can continue to operate through interactions with precipitation (moisture deficit) and include extremes that impact winter/spring flowering/fruiting phenology (late freeze). These indirect pathways could continue to complicate the rates and directions of population shifts. The weak responses to annual temperature trends indicate that seed production is not necessarily low at poleward population frontiers. Hump-shaped (convex) temperature response is not pervasive in the regions analyzed here. Several studies that could not be included in MASTIF (they do not reference seeds per tree) show strong seed production near poleward range limits in Quebec (Drobyshev *et al.*, 2014; Solarik *et al.*, 2020; Maleki

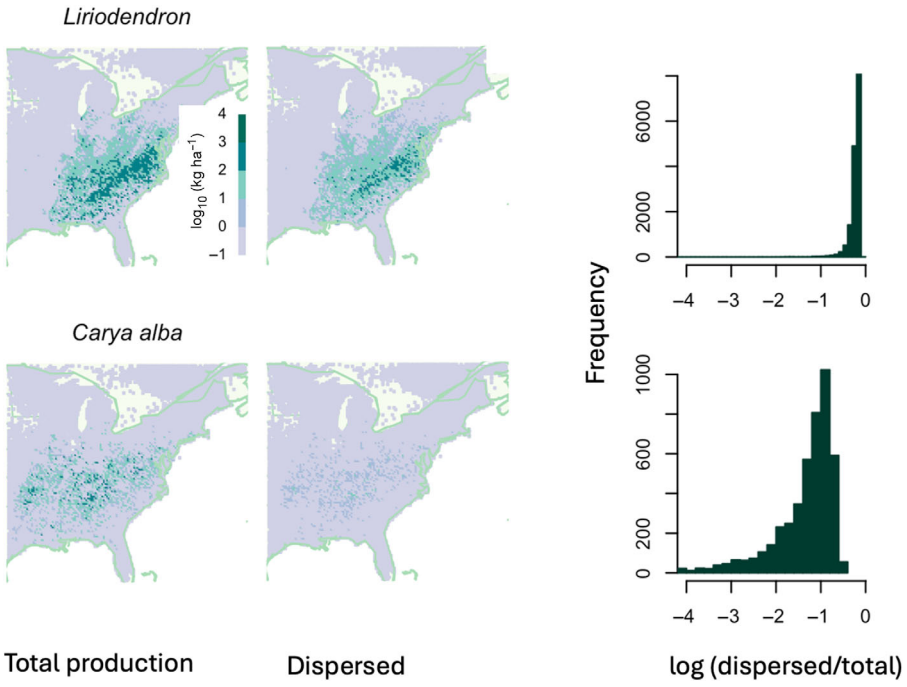

Fig. 8 Fraction of seed dispersed > 10 m in the absence of animal vectors for two species in North America (Fig. 3). Dispersal estimates come from the fitted dispersal kernel (Clark *et al*., 2019). Wind-dispersed *Liriodendron tulipifera* sends most seeds beyond 10 m, indicated by the dispersed map (center) that is much like the total (left) and as a log ratio of dispersed/total seed that is close to zero (dispersed = total, right). Large-seeded *Carya* sends a small fraction beyond 10 m.

et al., 2024), supporting the interpretation that temperature is not the dominant limitation on fecundity for most species.

Response velocity offers an alternative to traditional time-series methods when trends are buried in noise. The questions are not limited to mast production in trees (see also Clark *et al*., 2021). Response velocity also exposed the impact of habitat change on ground beetle abundances generated by noisy pitfall trap data (Qiu *et al*., 2023b). In such cases, the trend at a specific location is less important than the implications of change for species that vary in their climate sensitivities over regions. The time required for a local trend to emerge from noisy data may lag the indicators that can be extracted from response velocity.

Efforts to anticipate changes in food webs require understanding of bottom-up controls supported by fruit, seed, and nut production of trees (Rosenblatt & Schmitz, 2016). If mobile consumers such as insects, birds, and mammals outrun their resource base, then climate-change risk assessment has to consider not only trends in mean annual temperature but also its interactions with moisture and late freeze. Results here provide the estimates of food production per area available now and how it is changing. The disproportionate production of seeds, fruits, and nuts (Journe *et al*., 2022) and high density of frugivores (Terborgh, 1986; Schemske *et al*., 2009; Hargreaves *et al*., 2019) in the wet tropics both suggest impacts that could come through changes in bottom-up control.

For forest managers, results highlight the need to evaluate species responses to the multiple ways climate is changing, including interactions with terrain. In addition, to the mast production estimates needed by wildlife managers (MCSHEA *et al*., 2007), response velocity offers conservation and reforestation efforts that are currently guided by temperature-driven models (Gardner & Bullock, 2025) with the sensitivity that directly guides responses. These results have direct application to species-selection decisions that can be tailored to climate change and its interaction with local habitats.

Acknowledgements

We thank NEON for field support and, for data collection, William Schlesinger (Comstock Point, ME), Dale Brockway and Qinfeng Guo (longleaf pine), Janneke Hille Ris Lambers (Mount Ranier), Adrian Das (Sierra Nevada network), Jerry Franklin (Cascades), and Kristen Legg (Greater Yellowstone Ecosystem Study). In North America, funding came from the National Science Foundation and NASA, most recently NSF-DEB-2211764 to JSC, II, RK, EM, and MDR, and NASA (NASA-22-ECON22-0008) to JSC and TQ. European funding came from Ministère de l'Enseignement Supérieur de la Recherche et de l'Innovation, France, *Make Our Planet Great Again*, to JSC and GK. MB was funded by the European Union (ERC, ForestFuture, 101039066). We thank the Ministerio para la Transición Ecológica y el Reto Demográfico (MIITECO) for granting access to the Spanish National Forest Inventory.

Competing interests

None declared.

Author contributions

JSC designed and implemented sampling, modeling, computation, and wrote the manuscript. JSC, GK and TQ generated data sets and workflow. JSC, II, RK, EM and MDR contributed to the design of the most recent NSF grant. TB, MB, MC, JJC, SD, BF, AH-P, MEH, MH, LJ, VJ, JL, AM, SM, KM, TAN, EQ,

CDR, FR-S, M-CB-V, SV, MAZ, SZ and MZ contributed data and revisions.

ORCID

Taylar Bankston https://orcid.org/0000-0002-9798-7360
Michal Bogdziewicz https://orcid.org/0000-0002-6777-9034
Maxime Cailleret https://orcid.org/0000-0001-6561-1943
J. Julio Camarero https://orcid.org/0000-0003-2436-2922
James S. Clark https://orcid.org/0000-0002-5677-9733
Sylvain Delzon https://orcid.org/0000-0003-3442-1711
Bruno Fady https://orcid.org/0000-0003-2379-7617
Andrew Hacket-Pain https://orcid.org/0000-0003-3676-1568
Mick E. Hanley https://orcid.org/0000-0002-3966-8919
Inés Ibáñez https://orcid.org/0000-0002-1054-0727
Lauren Jenkins https://orcid.org/0000-0001-6537-575X
Valentin Journé https://orcid.org/0000-0001-7324-7002
Roland Kays https://orcid.org/0000-0002-2947-6665
Georges Kunstler https://orcid.org/0000-0002-2544-1940
Anders Mårell https://orcid.org/0000-0002-3328-4834
Sierra McMurry https://orcid.org/0009-0000-0268-8062
Emily Moran https://orcid.org/0000-0003-4624-1910
Thomas A. Nagel https://orcid.org/0000-0002-4207-9218
Tong Qiu https://orcid.org/0000-0003-4499-437X
Elena Quintero https://orcid.org/0000-0003-4979-6874
Miranda D. Redmond https://orcid.org/0000-0002-4657-7943
Francisco Rodriguez-Sánchez https://orcid.org/0000-0002-7981-1599
Samuel Venner https://orcid.org/0000-0001-7127-3733
Miguel A. Zavala https://orcid.org/0000-0003-1456-0132
Magdalena Zywiec https://orcid.org/0000-0002-5992-4051

Data availability

Code is available in R package MASTIF on CRAN. Data are deposited at the Duke Digital Repository https://research.repository.duke.edu/record/433?ln=en&v=tab.

References

Abatzoglou JT, Dobrowski SZ, Parks SA, Hegewisch KC. 2018. TerraClimate, a high-resolution global dataset of monthly climate and climatic water balance from 1958–2015. *Scientific Data* **5**: 170191.

Alquichire-Rojas S, Escobedo VM, González-Teuber M. 2024. Impacts of increased temperatures on floral rewards and pollinator interactions: a meta-analysis. *Frontiers in Plant Science* **15**: 8070.

Bourg NA, McShea WJ, Thompson JR, McGarvey JC, Shen X. 2013. Initial census, woody seedling, seed rain, and stand structure data for the SCBI SIGEO large forest dynamics plot. *Ecology* **94**: 2111–2112.

Bower AD, Frerker KL, Pike CC, Labonte NR, Palik BJ, Royo AA, Anderson SM, Ferreira AR, Brandt LA. 2024. A practical framework for applied forestry assisted migration. *Frontiers in Forests and Global Change* **7**: 4329.

Brito C, Dinis L-T, Moutinho-Pereira J, Correia CM. 2019. Drought stress effects and olive tree acclimation under a changing climate. *Plants* **8**: 232.

Charrier G, Martin-StPaul N, Damesin C, Delpierre N, ¤nninen HH, Torres-Ruiz JM, Davi H. 2021. Interaction of drought and frost in tree ecophysiology: rethinking the timing of risks. *Annals of Forest Science* **78**: 40.

Chen J, Hao Z, Guang X, Zhao C, Wang P, Xue L, Zhu Q, Yang L, Sheng Y, Zhou Y *et al.* 2019. Liriodendron genome sheds light on angiosperm phylogeny and species–pair differentiation. *Nature Plants* **5**: 18–25.

Clark JS. 1990. Landscape interactions among nitrogen mineralization, species composition, and long-term fire frequency. *Biogeochemistry* **11**: 1–22.

Clark JS, Andrus R, Arianoutsou M, Ascoli D, Bergeron Y, Bogdziewicz M, Boivin T, Bonal R, Caignard T, Cailleret M *et al.* 2026. Continental contrasts in climate extremes that control tree fecundity. *Global Change Biology* **32**: e70738.

Clark JS, Andrus R, Aubry-Kientz M, Bergeron Y, Bogdziewicz M, Bragg DC, Brockway D, Cleavitt NL, Cohen S, Courbaud B *et al.* 2021. Continent-wide tree fecundity driven by indirect climate effects. *Nature Communications* **12**: 1242.

Clark JS, Bell DM, Kwit M, Powell A, Zhu K. 2013. Dynamic inverse prediction and sensitivity analysis with high-dimensional responses: application to climate-change vulnerability of biodiversity. *Journal of Biological, Environmental, and Agricultural Statistics* **18**: 376–404.

Clark JS, Bell DM, Kwit MC, Zhu K. 2014. Competition-interaction landscapes for the joint response of forests to climate change. *Global Change Biology* **20**: 1979–1991.

Clark JS, LaDeau S, Ibanez I. 2004. Fecundity of trees and the colonization-competition hypothesis. *Ecological Monographs* **74**: 415–442.

Clark JS, Nuñez CL, Tomasek B. 2019. Foodwebs based on unreliable foundations: spatiotemporal masting merged with consumer movement, storage, and diet. *Ecological Monographs* **89**: e01381.

Corbet S, Fussell M, Ake R, Fraser A, Gunson C, Savage A, Smith K. 1993. Temperature and the pollinating activity of social bees. *Ecological Entomology* **18**: 17–30.

Cornes RC, van der Schrier G, Squintu AA. 2019. A reappraisal of the thermal growing season length across Europe. *International Journal of Climatology* **39**: 1787–1795.

Dobrowski SZ, Parks SA. 2016. Climate change velocity underestimates climate change exposure in mountainous regions. *Nature Communications* **7**: 12349.

Drobyshev I, Guitard M-A, Asselin H, Genries A, Bergeron Y. 2014. Environmental controls of the northern distribution limit of yellow birch in eastern Canada. *Canadian Journal of Forest Research* **44**: 720–731.

Feeley KJ, Silman MR. 2010. Biotic attrition from tropical forests correcting for truncated temperature niches. *Global Change Biology* **16**: 1830–1836.

Fei S, Desprez JM, Potter KM, Jo I, Knott JA, Oswalt CM. 2017. Divergence of species responses to climate change. Science. *Advances* **3**: e1603055.

Fernandez E, Mojahid H, Fadón E, Rodrigo J, Ruiz D, Egea JA, Ben Mimoun M, Kodad O, El Yaacoubi A, Ghrab M *et al.* 2022. Climate change impacts on winter chill in Mediterranean temperate fruit orchards. *Regional Environmental Change* **23**: 7.

Gardner CJ, Bullock JM. 2025. Revisiting the case for assisted colonisation under rapid climate change. *Journal of Applied Ecology* **62**: 1071–1077.

Gesch DB, Oimoen MJ, Greenlee SK, Nelson CA, Steuck MJ, Tyler DJ. 2002. The national elevation data set. *Photogrammetric Engineering and Remote Sensing* **68**: 5–11.

Gucci R, Lodolini EM, Rapoport HF. 2009. Water deficit-induced changes in mesocarp cellular processes and the relationship between mesocarp and endocarp during olive fruit development. *Tree Physiology* **29**: 1575–1585.

Hansen JE, Kharecha P, Sato M, Tselioudis G, Kelly J, Bauer SE, Ruedy R, Jeong E, Jin Q, Rignot E *et al.* 2025. Global warming has accelerated: are the united nations and the public well-informed? *Environment: Science and Policy for Sustainable Development* **67**: 6–44.

Hargreaves AL, Suárez E, Mehltreter K, Myers-Smith I, Vanderplank SE, Slinn HL, Vargas-Rodriguez YL, Haeussler S, David S, Muñoz J *et al.* 2019. Seed predation increases from the Arctic to the Equator and from high to low elevations. *Science Advances* **5**: eaau4403.

ISRIC. 2024. *World soil information.* SoilGrids. [WWW document] URL https://www.isric.org/ [accessed 1 June 2025].

Jenkins L, Borrero EQ, Bankston T, Hu M, Ibanez I, Kays R, Kunstler G, Luongo J, Sierra MM, Meyer K *et al.* 2026. Climate refugia in North American and European temperate forests: Local habitat and terrain conditions needed for tree fecundity. *Journal of Ecology.*

Journe V, Andrus R, Aravena M-C, Ascoli D, Berretti R, Berveiller D, Bogdziewicz M, Boivin T, Bonal R, Caignard T *et al.* 2022. Globally, tree fecundity exceeds productivity gradients. *Ecology Letters* **25**: 1471–1482.

Karger DN, Conrad O, Böhner J, Kawohl T, Kreft H, Soria-Auza RW, Zimmermann NE, Linder HP, Kessler M. 2017. Climatologies at high resolution for the earth's land surface areas. *Scientific Data* **4**: 170122.

Körner C, Hiltbrunner E. 2018. The 90 ways to describe plant temperature. *Perspectives in Plant Ecology, Evolution and Systematics* **30**: 16–21.

Le Roncé I, Gavinet J, Ourcival J-M, Mouillot F, Chuine I, Limousin J-M. 2021. Holm oak fecundity does not acclimate to a drier world. *New Phytologist* **231**: 631–645.

Lieffers VJ, Pinno BD, Beverly JL, Thomas BR, Nock C. 2020. Reforestation policy has constrained options for managing risks on public forests. *Canadian Journal of Forest Research* **50**: 855–861.

Lima JS, Lenoir J, Hylander K. 2024. Potential migration pathways of broadleaved trees across the receding boreal biome under future climate change. *Global Change Biology* **30**: e17471.

Linnakoski R, Kasanen R, Dounavi A, Forbes KM. 2019. Editorial: forest health under climate change: effects on tree resilience, and pest and pathogen dynamics. *Frontiers in Plant Science* **10**: 1157.

Loarie SR, Duffy PB, Hamilton H, Asner GP, Field CB, Ackerly DD. 2009. The velocity of climate change. *Nature* **462**: 1052–1055.

Losso A, Challis A, Gauthey A, Nolan RH, Hislop S, Roff A, Boer MM, Jiang M, Medlyn BE, Choat B. 2022. Canopy dieback and recovery in Australian native forests following extreme drought. *Scientific Reports* **12**: 21608.

MacKenzie WH, Mahony CR. 2021. An ecological approach to climate change-informed tree species selection for reforestation. *Forest Ecology and Management* **481**: 118705.

Maleki K, Marchand P, Charron D, Bergeron Y. 2024. Seedling recruitment in response to stand composition, interannual climate variability, and soil disturbance in the boreal mixed woods of Canada. *Journal of Vegetation Science* **35**: e13237.

Mcshea WJ, Healy WM, Devers P, Fearer T, Koch FH, Stauffer D, Waldon J. 2007. Forestry matters: decline of oaks will impact wildlife in hardwood forests. *The Journal of Wildlife Management* **71**: 1717–1728.

Meehl GA, Arblaster JM, Chung CTY. 2015. Disappearance of the southeast U.S. 'warming hole' with the late 1990s transition of the Interdecadal Pacific Oscillation. *Geophysical Research Letters* **42**: 5564–5570.

Moran EV, Clark JS. 2011. Estimating seed and pollen movement in a monoecious plant: a hierarchical Bayesian approach integrating genetic and ecological data. *Molecular Ecology* **20**: 1248–1262.

Muller-Landau HC, Wright SJ, Calderon O, Condit R, Hubbell SP. 2008. Interspecific variation in primary seed dispersal in a tropical forest. *Journal of Ecology* **96**: 653–667.

Nigro KM, Pelz K, Rocca ME, Redmond MD. 2025. Trailing edge contractions common in interior western US trees under varying disturbances. Nature. *Climate Change* **15**: 196–200.

Olson DM, Dinerstein E, Wikramanayake ED, Burgess ND, Powell GVN, Underwood EC, D'Amico JA, Itoua I, Strand HE, Morrison JC *et al.* 2001. Terrestrial ecoregions of the world: a new map of life on Earth. *Bioscience* **51**: 933–938.

Orain R, Lebreton V, Ermolli ER, Combourieu-Nebout N, Sémah AM. 2013. Carya as marker for tree refuges in southern Italy (*Boiano basin*) at the Middle Pleistocene. *Palaeogeography, Palaeoclimatology, Palaeoecology* **369**: 295–302.

Pederson N, Dyer JM, McEwan RW, Hessl AE, Mock CJ, Orwig DA, Rieder HE, Cook BI. 2014. The legacy of episodic climatic events in shaping temperate, broadleaf forests. *Ecological Monographs* **84**: 599–620.

Pesendorfer MB, Bogdziewicz M, Szymkowiak J, Borowski Z, Kantorowicz W, Espelta JM, Fernández-Martínez M. 2020. Investigating the relationship between climate, stand age, and temporal trends in masting behavior of European forest trees. *Global Change Biology* **26**: 1654–1667.

Qiu T, Aravena M-C, Ascoli D, Bergeron Y, Bogdziewicz M, Boivin T, Bonal R, Caignard T, Cailleret M, Calama R *et al.* 2023a. Masting is uncommon in trees that depend on mutualist dispersers in the context of global climate and fertility gradients. *Nature Plants* **9**: 1044–1056.

Qiu T, Bell AJ, Swenson JJ, Clark JS. 2023b. Habitat–trait interactions that control response to climate change: North American ground beetles (Carabidae). *Global Ecology and Biogeography* **32**: 987–1001.

Qiu T, Sharma S, Woodall CW, Clark JS. 2021. Niche shifts from trees to fecundity to recruitment that determine species response to climate change. *Frontiers in Ecology and Evolution* **9**: 9141.

Rabasa SG, Granda E, Benavides R, Kunstler G, Espelta JM, Ogaya R, Peñuelas J, Scherer-Lorenzen M, Gil W, Grodzki W *et al.* 2013. Disparity in elevational shifts of European trees in response to recent climate warming. *Global Change Biology* **19**: 2490–2499.

Rosenblad KC, Baer KC, Ackerly DD. 2023. Climate change, tree demography, and thermophilization in western US forests. *Proceedings of the National Academy of Sciences, USA* **120**: e2301754120.

Rosenblatt AE, Schmitz OJ. 2016. Climate change, nutrition, and bottom-up and top-down food web processes. *Trends in Ecology & Evolution* **31**: 965–975.

Schemske DW, Mittelbach GG, Cornell HV, Sobel JM, Roy K. 2009. Is there a latitudinal gradient in the importance of biotic interactions? *Annual Review of Ecology, Evolution, and Systematics* **40**: 245–269.

Schliep EM, Gelfand AE, Clark JS. 2015. Stochastic modeling for velocity of climate change. *Journal of Agricultural, Biological, and Environmental Statistics* **20**: 323–342.

Sharma S, Andrus R, Bergeron Y, Bogdziewicz M, Bragg DC, Brockway D, Cleavitt NL, Courbaud B, Das AJ, Dietze M *et al.* 2022. North American tree migration paced by climate in the West, lagging in the East. *Proceedings of the National Academy of Sciences, USA* **119**: e2116691118.

Shibata M, Masaki T, Yagihashi T, Shimada T, Saitoh T. 2020. Decadal changes in masting behaviour of oak trees with rising temperature. *Journal of Ecology* **108**: 1088–1100.

Sittaro F, Paquette A, Messier C, Nock CA. 2017. Tree range expansion in eastern North America fails to keep pace with climate warming at northern range limits. *Global Change Biology* **23**: 3292–3301.

Solarik KA, Cazelles K, Messier C, Bergeron Y, Gravel D. 2020. Priority effects will impede range shifts of temperate tree species into the boreal forest. *Journal of Ecology* **108**: 1155–1173.

Stephenson AG. 1981. Flower and fruit abortion: proximate causes and ultimate functions. *Annual Review of Ecology, Evolution, and Systematics* **12**: 253–279.

Suzuki W, Osumi K, Masaki T. 2005. Mast seeding and its spatial scale in Fagus crenata in northern Japan. *Forest Ecology and Management* **205**: 105–116.

Terborgh J. 1986. *Community aspects of frugivory in tropical forests.* Dordrecht, the Netherlands: Springer.

Thomashow MF. 1999. Plant cold acclimation: freezing tolerance genes and regulatory mechanisms. *Annual Review of Plant Biology* **50**: 571–599.

Thornton M, Shrestha R, Wei Y, Thornton P, Kao S-C, Wilson B. 2022. *Daymet: daily surface weather data on a 1-km grid for North America, v.4 R1.* [WWW document] URL https://daac.ornl.gov/cgi-bin/dsviewer.pl?ds_id=2129.

USDA Forest Service. 2022. *National forest system reforestation strategy growing and nurturing resilient forests.* Washington, DC, USA: Department of Agriculture.

Whipple AV, Cobb NS, Gehring CA, Mopper S, Flores-Rentería L, Whitham TG. 2019. Long-term studies reveal differential responses to climate change for trees under soil- or herbivore-related stress. *Frontiers in Plant Science* **10**: 132.

Williams MI, Dumroese RK. 2013. Preparing for climate change: forestry and assisted migration. *Journal of Forestry* **111**: 287–297.

Wion AP, Weisberg PJ, Pearse IS, Redmond MD. 2020. Aridity drives spatiotemporal patterns of masting across the latitudinal range of a dryland conifer. *Ecography* **43**: 569–580.

Woodall CW, Oswalt CM, Westfall JA, Perry CH, Nelson MD, Finley AO. 2009. An indicator of tree migration in forests of the eastern United States. *Forest Ecology and Management* **257**: 1434–1444.

Wright MC, van Mantgem P, Stephenson NL, Das AJ, Keeley JE. 2021. Seed production patterns of surviving Sierra Nevada conifers show minimal change following drought. *Forest Ecology and Management* **480**: 118598.

Wyckoff P, Clark J. 2002. The relationship between growth and mortality for seven co-occurring tree species in the southern Appalachian Mountains. *Journal of Ecology* **90**: 604–615.

Zhu K, Woodall C, Clark J. 2012. Failure to migrate: Lack of tree range expansion in response to climate change. *Global Change Biology* **18**: 1042–1052.

Zhu K, Woodall CW, Ghosh S, Gelfand AE, Clark JS. 2014. Dual impacts of climate change: forest migration and turnover through life history. *Global Change Biology* **20**: 251–264.

Supporting Information

Additional Supporting Information may be found online in the Supporting Information section at the end of the article.

Dataset S1 Model fitting, sample sizes, and diagnostics.

Dataset S2 Posterior mean estimates.

Dataset S3 Posterior standard errors.

Fig. S1 Distribution of observations in MASTIF restricted to the last 15 yr that are used in this analysis.

Fig. S2 The prediction grid consists of 205 125 inventory plots in North America and 177 174 in Europe.

Fig. S3 Study species by genus and family include woody gymnosperms and angiosperms.

Fig. S4 Response velocity for each species grouped by genus in North America.

Fig. S5 Response velocity for each species grouped by genus in Europe.

Table S1 Phylogenetic signal for five indices, with significant values ($P < 0.05$) in bold font.

Table S2 Species on North American inventory plots, with plot numbers, mean response velocity, and spread of rates across the map (95% interval).

Table S3 Species on European inventory plots, with plot numbers, mean response velocity, and spread of rates across the map (95% interval).

Table S4 Metadata for file datasetS1.csv.

Table S5 Metadata for files datasetS2.csv and datasetS3.csv.

Please note: Wiley is not responsible for the content or functionality of any Supporting Information supplied by the authors. Any queries (other than missing material) should be directed to the *New Phytologist* Central Office.